Hindawi
International Journal of Photoenergy
Volume 2019, Article ID 4616198, 8 pages
https://doi.org/10.1155/2019/4616198

Research Article

TD-DFT Investigations on Optoelectronic Properties of Fluorescein Dye Derivatives in Dye-Sensitized Solar Cells (DSSCs)

Juma Mzume Juma, Said Ali H. Vuai, and N. Surendra Babu

Department of Chemistry, College of Natural and Mathematical Science, The University of Dodoma, P. O. Box 338 Dodoma, Tanzania

Correspondence should be addressed to Said Ali H. Vuai; saidhamadv@yahoo.co.uk

Received 24 May 2018; Revised 30 August 2018; Accepted 23 September 2018; Published 8 January 2019

Academic Editor: Leonardo Palmisano

This research work was conducted to investigate the structural, molecular, electronic, and photophysical parameters of the fluorescein dye derivatives using the density functional theory (DFT) and time dependent-density functional theory (TD-DFT) computations. The organic donor-π-acceptor dye used for dye-sensitized solar cells, based on 2-(3-hydroxy-6-oxo-6H-xanthene-9-yl)benzoic acid (fluorescein) and its five derivatives, was investigated. The derivatives were formed by attaching different donor groups at para position. The excited state energies, electron absorption spectra, and oscillator strengths (f) were calculated using TD-DFT/B3LYP/6-311G basis set calculations on fully DFT-optimized geometries. The HOMO orbital, LUMO orbital, and energy gap values show that fluorescein attached with thiophene (FST) compound has a smaller energy gap compared to others and the fluorescein attached with an amine (FSA) have a larger energy gap than all compounds. The increasing order of the energy gap between HOMO and LUMO for the fluorescein and its derivatives is FST < FSE < FSM < FS < FSO < FSA. In terms of electron injection efficiency, it was found that the FST has higher electron injection efficiency compared with other derivatives. In addition, light-harvesting efficiencies (LHEs) were calculated and the results showed that the FST has the highest LHE value. It is therefore suggested that FST has better properties for application in DSSC according to the result obtained.

1. Introduction

Steadily increasing global demand for energy coupled with depletion of harmful environmental effects associated with combustion of fossil fuels has necessitated the rapid development of renewable energy technologies [1, 2]. Dye-sensitized solar cells (DSSCs) have received considerable attention due to the fascinating low cost of the conversion of photovoltaic energy compared to the silicon-based semiconductor solar cell [3, 4]. Particularly, DSSCs are composed of a wide-bandgap semiconductor, the sensitizer (dye molecules), a transparent conductive oxide layer (TCO), and redox electrolyte (typically iodide/triiodide) [5]. The dye captures solar radiation in the visible region of the spectrum and excites the electron into the conductive band of the semiconductor; finally, an electron is regenerated to the dye by the redox electrolyte.

Up to now, DSSCs as reported by Mathew et al. have certified recorded efficiencies of about 13% for the metal organic dye complex on the basis of nanostructured titanium oxide (TiO_2) film sensitized by zinc porphyrin (SM 315) under full sun illumination at the laboratory scale device [6]. Metal-free organic dyes have recently received more attention than metal organic dye complexes. This is due to their low toxicity, high molar extinction coefficient, easy accessibility, light weight, and cost effectivity [1]. Accordingly, researchers make effort on the synthesis of metal-free organic dye for dye-sensitized solar cell application. Unfortunately, they have narrow optical absorption spectra, which hinder the maximum short-circuit current density (J_{sc}) to be achieved and therefore results into relatively lower power conversion efficiency (9.5%) [7].

The general structure of metal-free organic dyes contains a donor-pi-acceptor system. The intramolecular charge

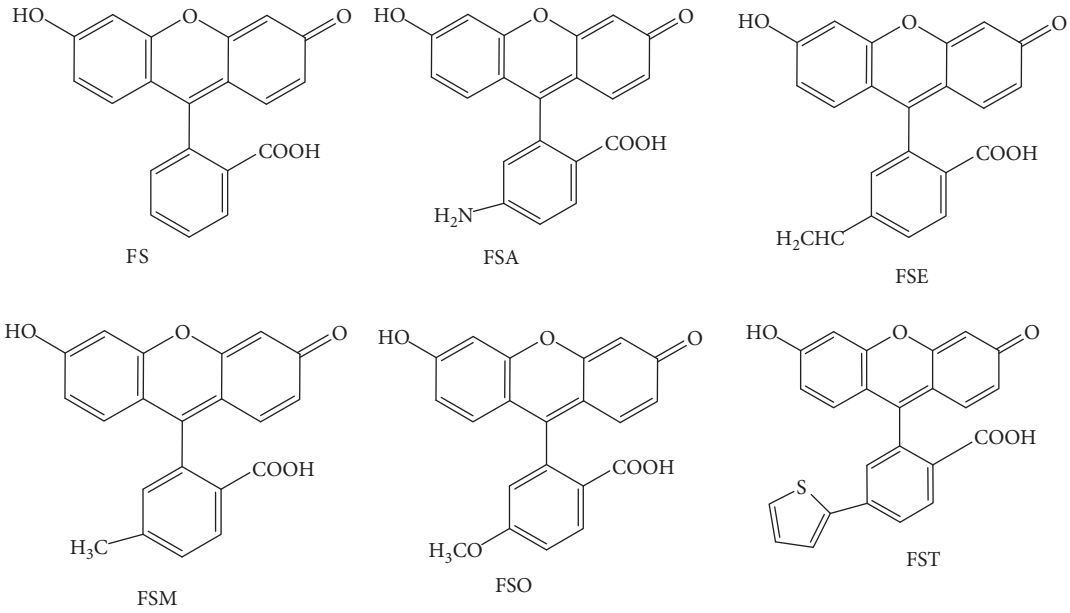

Figure 1: Chemical structures of fluorescein and its derivatives.

transfer (ICT) from the donor to acceptor at the photoexcitation injects photoelectron into the conduction band of the semiconductor through the electron accepting group at the anchoring unit. By changing the electron donor, acceptor, and π-spacer, the HOMO and LUMO energies are affected [4, 7–13]. The fluorescein is a coplanar compound, and the electron-accepting group is attached heterocyclic due to the electron-withdrawing group carbonyl (C=O) of carboxylic acid for accepting an electron from the electron donor.

Fluorescein dye has been used in DSSC with the highest reported power conversion efficiency of 6.54% [8]. It is possible to modify the structure of fluorescein by increasing the power conversion efficiency through attaching of the donating group that increases the transition of an electron as well as absorption spectra of the dye [4]. When the LHE, electron injection, and electron regeneration are high, the short-circuit current density becomes high hence increases power conversion efficiency. The aim of this study was to investigate the power conversion efficiency of modified fluorescein dyes for application in the dye-sensitized solar cell.

2. Methodology

Fluorescein and its five derivatives were investigated. The derivatives were obtained by attaching donor group para to the acceptor group (carboxylic acid). The derivatives that were investigated are fluorescein (FS), fluorescein doped with an amine group (FSA), fluorescein doped with ethene (FSE), fluorescein doped with methane (FSM), fluorescein doped with methoxy (FSO), and fluorescein doped with thiophene (FST). Chemical structures of the molecules are shown in Figure 1. All calculations for structural optimization were done by using the DFT/B3LYP method with 6-311G basis set and were calculated in gas and solvent phases. The density functional theory (DFT) and time-dependent density functional theory (TD-DFT) with the B3LYP (Becke three-parameter Lee-Yang-Parr) method [9] and 6-311G basis set were used. The excited state energies, electron absorption spectra, and oscillator strengths (f) were investigated using the TD-DFT/B3LYP method with 6-311G basis set after optimization [5] in gas and solvent phases. All calculations in the solvent phase adopted the polarizable continuum model (PCM) [10]. The solvent that was used for these calculations was acetonitrile. The HOMO and LUMO levels were calculated by using D-DFT/B3LYP. Generally, all calculations were performed using the Gaussian 09 software and the models of electron density of various energy levels were visualized using GaussView Version 5.0 [6].

3. Results and Discussion

3.1. Geometry Structures Optimized. The optimized structures of all studied compounds are illustrated in Figure 2. The total energy (E_T) after optimization was −31198.88, −32705.41, −33304.93, −32268.72, −34314.97, and −46213.36 eV for FS, FSA, FSE, FSM, FSO, and FST, respectively, as shown in Table 1. The optimized geometries of all studied dyes showed that they have similar coplanar conformation. This means that the coplanar molecular structure can improve the electron transfer from the donor to the acceptor through the π-spacer [11].

3.2. Frontier Molecular Orbitals (FMO). The most important characteristic of the metal-free organic dye is the intramolecular charge transfer (ICT) from the donor to the anchoring group through the π-bridge. This feature can be affected by the energy gap of the molecule that also affects the photocurrent.

Table 1 illustrates the values of HOMO and LUMO orbitals, energy gap, dipole moment, and total energies of each studied molecule in electron volt (eV). All HOMOs showed typical aromatic features with electron delocalization

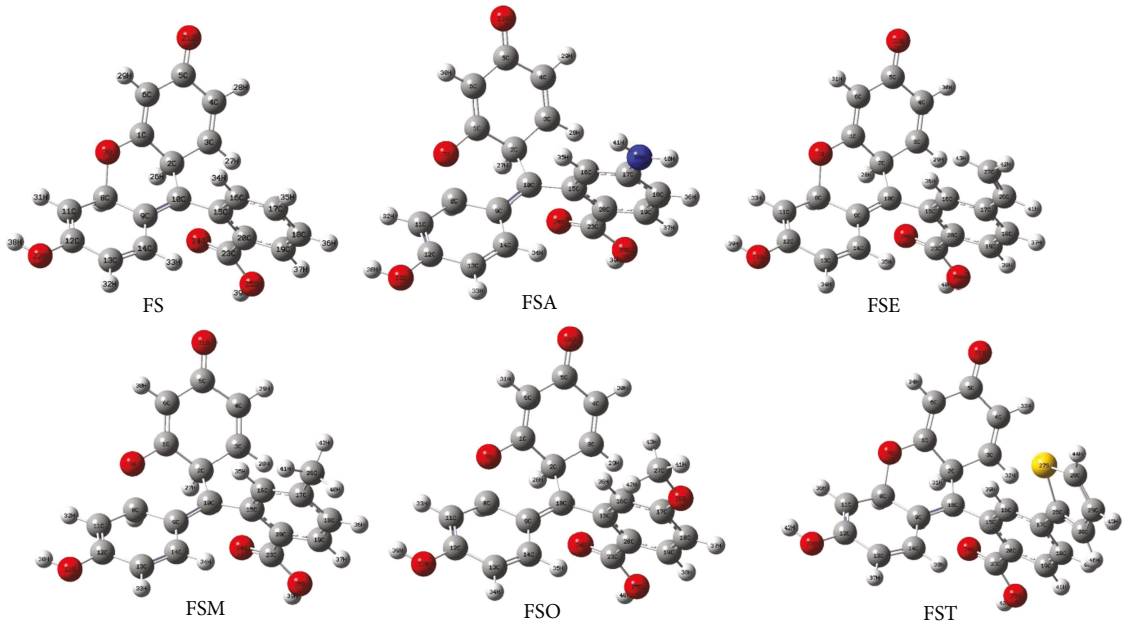

Figure 2: Optimized geometries of the studied molecules in a solvent phase.

Table 1: Electrical and optical parameters for all studied compounds obtained in a solvent phase.

Compounds	E_{HOMO} (eV)	E_{LUMO} (eV)	E_T (eV)	E_g (eV)	μ (debye)
FS	−6.164	−2.248	−31198.88	3.916	9.8233
FSA	−6.108	−2.091	−32705.41	4.017	9.7597
FSE	−6.164	−2.420	−33304.93	3.744	9.5789
FSM	−6.155	−2.204	−32268.72	3.951	9.6031
FSO	−6.168	−2.179	−34314.97	3.989	8.2833
FST	−6.171	−2.496	−46213.36	3.675	10.681

for the whole conjugated molecule [13]. The LUMOs are mainly concentrated on the electron deficient unit and the right of the molecule chain. HOMO orbital of molecules presents a bonding character, while the LUMO orbital presents an antibonding character. The HOMO and LUMO orbitals are shown in Figure 3.

Normally, the molecules having a large dipole moment have strong asymmetry in the distribution of electronic charge and can be more reactive and sensitive to external electric field [11]. From the results, it can be observed that the dipole moment of the FST molecule is greater than the other derivatives by implying high sensitivity. Also, the electric dipole moment with electron absorption spectra helps to detect the occurrence of the charge transfer from the donor to acceptor upon the photoexcitation. On the other hand, the strong electron-donating group results into a high HOMO energy level [5]. The HOMO energy levels for the studied dyes are in order: FST > FSO > FS > FSE > FSM > FSA. The high value of the FST dye molecule is attributed to the presence of a conjugated double bond in the thiophene.

3.3. Energy Gap (E_g). The energy gap is the energy difference between the highest occupied molecular orbital (HOMO) and the lowest unoccupied molecular orbital (LUMO). Normally, the smaller energy gap of the compound results in ease of transporting electrons from HOMO to LUMO levels through absorption of light energy with an appropriate wavelength [5]. The results showed that (Table 1) the FST dye derivative has the lowest energy gap compared to the other dye derivatives. This means that the transfer of an electron from HOMO to LUMO occurs easily. It is therefore suggested that FST is good for application in DSSC compared with other studied dye derivatives.

3.4. Photovoltaic Properties

3.4.1. Theoretical Background. The power conversion efficiency is the percentage of the solar energy shining on a solar cell device that is converted into usable electricity. The power conversion efficiency (η) was calculated as follows:

$$\eta = \mathrm{FF}\frac{V_{oc}J_{sc}}{P_{inc}}, \tag{1}$$

where P_{inc} is the incident power density, J_{sc} is the short-circuit current, V_{oc} is the open-circuit voltage, and FF denotes the fill factor. To analyze the relationship between

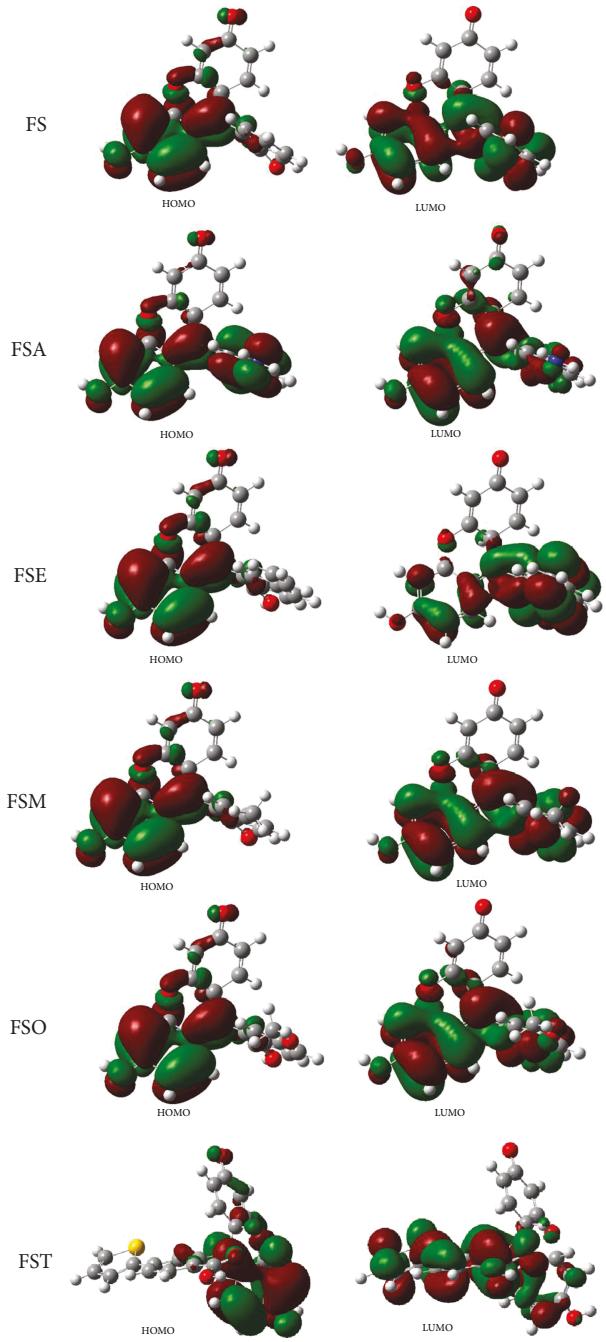

Figure 3: The HOMO and LUMO orbitals of the studied dye molecules.

V_{oc} and E_{LUMO} of the dyes based on electron injection (in DSSCs) from LUMO to the conduction band of semiconductor TiO_2 (E_{CB}), the energy relationship can be expressed [12] as follows:

$$V_{oc} = E_{LUMO} - E_{CB}. \quad (2)$$

From the studied dye derivatives, the values of V_{oc} were calculated according to the equation (2) which range from 1.0535 eV to 1.4955 eV as shown in Table 2. These values are sufficient for a possible efficient electron injection.

The short-circuit current density (J_{sc}) in DSSCs is determined by the following equation [4]:

$$J_{sc} = \int \mathrm{LHE}(\lambda)\Phi_{inject}\eta_{collect}d\lambda, \quad (3)$$

where $\mathrm{LHE}(\lambda)$ is the light-harvesting efficiency at a given wavelength, Φ_{inject} is the electron injection efficiency, and $\eta_{collect}$ denotes the charge collection efficiency. In the system where there are only differences in dye, $\eta_{collect}$ can be assumed to be constant. The LHE can be calculated through the following equation:

$$\mathrm{LHE} = 1 - 10^{-f}, \quad (4)$$

where f is the oscillator strength of adsorbed dye molecules.

Φ_{inject} is related to the driving force (ΔG_{inject}) of electrons injecting from the excited states of dye molecules to the semiconductor (conduction band). It can be estimated as follows [13]:

$$\Delta G_{inject} = E_{OX}^{dye*} - E_{CB}^{TiO_2} = E_{OX}^{dye} + E_{0-0}^{dye} - E_{CB}^{TiO_2}. \quad (5)$$

From the equations (1), (2), (3), (4), and (5), we could predict theoretically the efficiency of novel dyes without intensive calculations.

In the above equations, E_{OX}^{dye*} is the oxidation potential of the excited dye, E_{OX}^{dye} is the oxidation potential of the ground state of the dye, E_{0-0}^{dye} is the vertical transition energy, and $E_{CB}^{TiO_2}$ is the conduction band edge of the TiO_2 semiconductor. So, J_{sc} can be well estimated through LHE and ΔG_{inject}.

Two models can be used for the evaluation of E_{OX}^{dye*} [14]. The first implies that the electron injection occurs from the unrelaxed excited state. For this reaction path, the excited state oxidation potential can be extracted from the redox potential of the ground state, E_{OX}^{dye}, which was calculated at the B3LYP-6-31G(d) approach and the vertical transition energy corresponding to the photoinduced intermolecular charge transfer (ICT):

$$E_{OX}^{dye*} = E_{OX}^{dye} - \lambda_{max}^{ICT}, \quad (6)$$

where λ_{max}^{ICT} is the energy of the ICT. Note that this relation is only valid if the entropy change during the light absorption process can be neglected. For the second model, one assumes that electron injection occurs after relaxation. Given this condition, E_{OX}^{dye} is expressed as follows [15]:

$$E_{OX}^{dye*} = E_{OX}^{dye} - E_{0-0}^{dye}. \quad (7)$$

3.4.2. Electron Injection. The description of the electron transfer from a dye to a semiconductor and the rate of the

Table 2: Photovoltaic properties of dyes in a solvent phase.

Dyes	E_{OX}^{dye} (eV)	E_{OX}^{dye*} (eV)	ΔG_{inject} (eV)	LHE	V_{oc} (eV)	$\lvert V_{RP}\rvert$ (eV)
FS	6.163	2.814	−1.186	0.13	1.752	1.081
FSA	6.108	2.648	−1.352	0.25	1.909	1.054
FSE	6.164	2.984	−1.016	0.15	1.58	1.082
FSM	6.155	2.745	−1.255	0.16	1.796	1.077
FSO	6.168	2.698	−1.302	0.19	1.821	1.084
FST	6.171	3.051	−0.949	0.62	1.504	1.085

charge transfer process can be derived from the general classical Marcus theory [16–18].

$$k_{inject} = |V_{RP}|(2/h(\pi/\lambda k_B T))1/2 \exp\left[-\left(\Delta G_{inject} + \lambda\right)2/4\lambda k_B T\right]. \quad (8)$$

In equation (8), k_{inject} is the rate constant (in s^{-1}) of the electron injection from dye to TiO_2, k_B is the Boltzmann thermal energy, h is the Planck constant, G_{inject} is the free energy of injection, and $|V_{RP}|$ is the coupling constant between the reagent and the product potential curves. Equation (8) revealed that larger $|V_{RP}|$ leads to higher rate constant which would result in a better sensitizer. The use of the generalized Mulliken-Hush (GMH) formalism allows evaluating $|V_{RP}|$ for a photoinduced charge transfer [16]. It was explained that $|V_{RP}|$ can be evaluated as follows [17]:

$$|V_{RP}| = \frac{\Delta E_{RP}}{2}. \quad (9)$$

The injection driving force can be formally expressed within Koopmans approximation as

$$\Delta E_{RP} = \left[E_{LUMO}^{dye} + 2E_{HOMO}^{dye}\right] - \left[E_{LUMO}^{dye} + E_{HOMO}^{dye} + E_{CBO}^{TiO_2}\right], \quad (10)$$

where $E_{CBO}^{TiO_2}$ is the conduction band edge. It is difficult to accurately determine $E_{CBO}^{TiO_2}$ because it is highly sensitive to the operating conditions (e.g., the pH of the solution). Thus, we have used $E_{CBO}^{TiO_2} = -4.0\,eV$ [18] which is an experimental value corresponding to conditions where the semiconductor is in contact with aqueous redox electrolytes of fixed pH 7.0 [19, 20].

More quantitatively, for a closed-shell system, E_{LUMO}^{dye} corresponds to the reduction potential of the dye E_{RED}^{dye}, whereas the HOMO energy is related to the potential of the first oxidation (i.e., $E_{HOMO}^{dye} = E_{OX}^{dye}$). As a result, equation (7) becomes

$$\Delta E_{RP} = \left[E_{OX}^{dye} + E_{OX}^{TiO_2}\right]. \quad (11)$$

According to Koopman's theory, the ground state oxidation potential energy is related to ionization energy [21].

The photovoltaic properties λ_{max}, ΔG_{inject}, $E_{OX}^{dye}E_{OX}^{dye*}\lambda_{max}^{ICT}$, and LHE were presented in Table 2. The short-circuit current (J_{sc}) depends on two main influencing factors: light-harvesting efficiency (LHE) and the electronic injection free energy (ΔG_{inject}) (equation (3)). The LHE is considered as a very important factor for the organic dyes in which we could appreciate the role of the dyes in the DSSC, i.e., absorbing photons and injecting photoexcited electrons to the conduction band of the semiconductor (TiO_2). In order to know what to give an intuitional impression of the influence of the donor spacer of the LHE, we simulated the UV/Vis absorption spectra of the six dyes. We observed that in a different dye, the oscillator strengths were changed. As shown in Table 2, the LHE of the dyes falls within the range of 0.13–0.62.

From Table 2, ΔG_{inject} is negative for all studied dyes. This reveals that the electron injection process is spontaneous [11] and dye's excited state would be located above the conduction band edge of TiO_2 resulting in a favorable condition for electron injection. Among these six dyes, it was observed that the dye FST has the larger ΔG_{inject}. Based just on LHE and ΔG_{inject} related to J_{sc} [5], we could conclude that the cell containing the FST dye should have the highest J_{sc} due to its relatively large LHE and injection driving force compared to the other dyes.

From the calculation, it is revealed that FST has the largest electron injection value compared to the rest of the molecules due to their π-bond in the donor group. Conversely, FSA has the smallest electron injection because of NH_2 as a donating group. With regard to light-harvesting efficiency which is responsible for power conversion efficiency, the higher the LHE is, the higher the power conversion efficiency will be. From the calculation, it was observed that the FST has greater LHE and the FS has the smallest LHE as shown in Table 2.

3.5. Absorption Properties. The computed oscillator strength, transition energy (HOMO to LUMO) level, and vertical excited singlet state of all studied dye molecules in an acetonitrile solvent and gas media are tabulated in Table 3. During the calculation, the first and the third excitation showed the larger oscillator strength for most of the studied dye molecules.

The first vertical excited energy of all studied dyes increased depending on the donating group: FST < FSE < FS < FSM < FSA < FSO (3.117 < 3.1768 < 3.3537 < 3.4097 <

Table 3: The absorption properties of studied dye derivatives in a gas phase and acetonitrile.

Dyes	In gas				Acetonitrile			
	λ_{max} (nm)	λ in eV	f	Transition	λ_{max} (nm)	λ in eV	f	Transition
FS	390.56	3.1749	0.0253	H → L (93.65%)	**369.69**	**3.3537**	**0.0587**	**H → L (89.41%)**
	370.13	3.3501	0.0003	H → L + 1 (59.58%)	353.13	3.5110	0.0071	H → L + 2 (36.25%)
	362.23	3.4232	0.0004	H → L + 1 (75.57%)	338.02	3.6680	0.0326	H → L + 3 (50.90%)
	347.56	3.5677	0.0003	H → L (7.55%)	331.28	3.7426	0.0391	H → L + 6 (77.12%)
	355.00	**3.7014**	**0.0528**	**H → L + 4 (68.92%)**	322.26	3.8473	0.0084	H → L (84.67%)
	327.74	3.7834	0.0359	H → L + 2 (68.24%)	294.05	4.2164	0.0190	H → L (61.20%)
FSA	368.51	3.3645	0.0003	H → L (93.65%)	358.71	3.4564	0.0265	H → L + 1 (51.255)
	353.18	**3.5105**	**0.0589**	**H → L + 1 (59.58%)**	353.73	3.5050	0.0061	H → L + 3 (40.31%)
	344.24	3.6017	0.0129	H → L + 1 (75.57%)	**347.68**	**3.5661**	**0.1224**	**H → L + 1 (43.32%)**
	328.30	3.7765	0.0214	H → L (75.55%)	337.03	3.6787	0.0015	H → L (53.01%)
	322.93	3.8393	0.0099	H → L + 4 (68.92%)	334.65	3.7049	0.0034	H → L (69.58%)
	320.89	3.8638	0.0403	H → L + 2 (68.24%)	317.79	3.9015	0.0015	H → L (47.99%)
FSE	413.62	2.9975	0.0175	H → L (96.79%)	390.28	3.1768	0.0348	H → L (96.88%)
	376.73	3.2911	0.0003	H → L + 1 (82.35%)	353.17	3.5107	0.0072	H → L (8.44%)
	369.83	3.3524	0.0002	H → L + 1 (60.45%)	**339.32**	**3.6539**	**0.0715**	**H → L + 3 (64.09%)**
	365.92	3.3883	0.0007	H → L (83.19%)	333.98	3.7123	0.0245	H → L + 4 (59.45%)
	340.06	3.6460	0.0362	H → L + 2 (51.62%)	329.51	3.7627	0.0174	H → L (77.87%)
	331.56	**3.7394**	**0.0603**	**H → L + 1 (50.53%)**	305.32	4.0608	0.0159	H → L + 2 (77.38%)
FSM	**380.31**	**3.2601**	**0.0312**	**H → L (91.99%)**	**363.62**	**3.4097**	**0.0734**	**H → L (87.53%)**
	369.63	3.3542	0.0003	H → L + 1 (62.35%)	353.22	3.5102	0.0068	H → L + 3 (43.93%)
	356.67	3.4762	0.0004	H → L + 1 (75.19%)	337.68	3.6716	0.0220	H → L + 3 (46.64%)
	340.47	3.6416	0.0018	H → L (67.27%)	329.93	3.7579	0.0388	H → L + 3 (81.16%)
	331.97	3.7348	0.0312	H → L + 3 (69.98%)	320.76	3.8653	0.0087	H → L (86.85%)
	323.65	3.8309	0.0205	H → L + 2 (77.57%)	290.22	4.2721	0.0308	H → L + 2 (53.75%)
FSO	369.67	3.3539	0.0002	H → L + 1 (60.73%)	**357.42**	3.4689	**0.0887**	**H → L (85.79%)**
	364.34	3.4030	0.0413	H → L (84.62%)	353.14	3.5109	0.0134	H → L + 3 (46.22%)
	349.72	3.5452	0.0004	H → L + 1 (72.09%)	337.35	3.6752	0.0291	H → L (40.51%)
	333.54	3.7172	0.0261	H → L + 3 (48.88%)	327.72	3.7832	0.0059	H → L+3 (82.29%)
	326.48	**3.7977**	**0.0496**	H → L (65.11%)	319.92	3.8754	0.0093	H → L (87.05%)
	314.74	3.9392	0.0095	H → L + 2 (77.57%)	302.13	4.1036	0.0249	H → L (88.61%)
FST	421.81	2.9394	0.0196	H → L (96.87%)	397.74	3.1173	0.0360	H → L (97.64%)
	383.62	3.2319	0.0007	H → L + 1 (86.15%)	353.20	3.5104	0.0121	H → L + 1 (41.14%)
	373.16	3.3225	0.0008	H → L (86.70%)	**343.16**	**3.6130**	**0.4195**	H → L + 1 (54.56%)
	369.95	3.3513	0.0002	H → L (63.24%)	338.17	3.6663	0.1284	H → L + 3 (32.36%)
	341.76	**3.6278**	**0.0627**	H → L + 3 (47.86%)	334.76	3.7036	0.0086	H → L + 4 (42.69%)
	334.78	3.7035	0.2335	H → L + 2 (38.95%)	330.99	3.7459	0.0657	H → L + 1 (48.39%)

The bolded values in Table 3 indicate the highest value of oscillator strength with respect to the calculated the λ_{max} (nm), excitation energies (eV), oscillator strengths (f), assignment of molecular orbital contributions, and character.

3.4564 < 3.4689). It is revealed that the more the conjugation of the donor group the higher the vertical excitation energy [3–11]. The excitation energy of all dyes is higher in acetonitrile solvent than that in the gas phase. The transition (HOMO to LUMO) characters in acetonitrile solvent and gas phase are different. This is due to the effect of the polar environment resulted by acetonitrile [5].

On the other hand, the maximum wavelength (λ_{max}) in a gas phase differs from that of the solvent phase (acetonitrile) as indicated in Figures 3–5. The oscillator strength also increases in the solvent phase through the addition of acetonitrile in the studied molecules.

The decrease in absorption wavelength (UV-Vis) in the solvent phase (Figure 4) is due to the addition of polar solvent [5]. The absorption wavelengths of FS, FSA, FSE, FSM, FSO, and FST in gas and solvent phases are 390.52, 368.51, 413.62, 380.31, 369.67, and 421.81 and 369.69, 358.71, 390.28, 363.62, 357.42, and 397.74, respectively. The FST derivative has higher maximum wavelength than the other derivatives in both gas and solvent phases. This is a

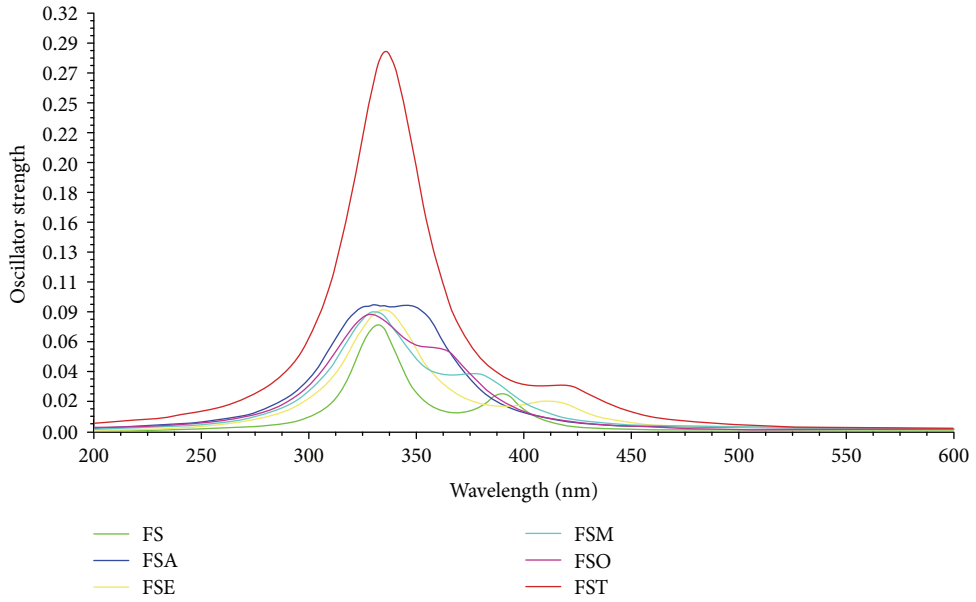

Figure 4: The maximum wavelength and oscillator strength of all fluorescein dye derivatives in the gas phase.

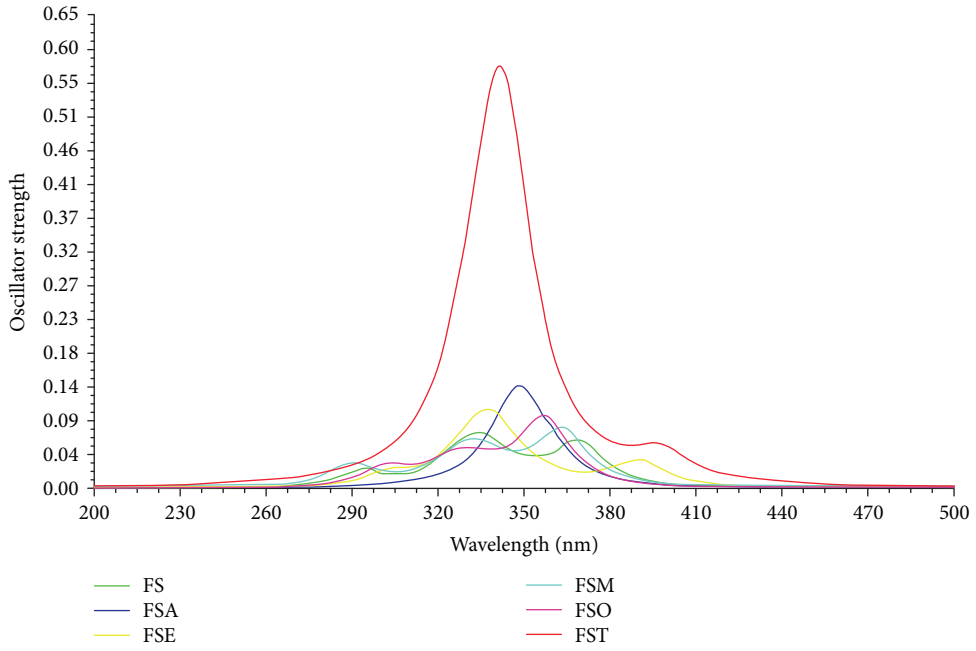

Figure 5: The maximum wavelength and oscillator strength of all fluorescein dye derivatives in the solvent phase.

result of increasing the number of conjugated double bonds in the FST. Generally, the number of conjugated double bonds always increases the absorption spectra of the molecule [4].

4. Conclusion

The modification of the chemical structures of the five fluorescein dye derivatives was done in order to improve the electronic and optical properties of the studied dyes. It was observed that the molecule with high conjugated double bonds has both high absorption spectra and increased electron injection efficiency. It was further revealed that the conjugation makes the bandgap decreased due to the increase of the absorption wavelengths. Therefore, the investigation shows that FST is better for application in DSSC in comparison to other derivatives due to the presence of large wavelength, high LHE, high electron injection efficiency, and the small bandgap. On the other hand, the LUMO energy levels of all studied dye molecules are higher than that of the

conduction band of the semiconductor (TiO_2). This criterion is important for photoexcited electron transfer from the dye to the semiconductor (TiO_2).

Data Availability

The data used to support the findings of this study are available from the corresponding author upon request.

Conflicts of Interest

No potential conflicts happened in conducting our research.

Acknowledgments

This work has been completed with funding from the Zanzibar Higher Education Loans Board (ZHELB). The authors acknowledge the ZHELB for the financial support they provided to undertake the master degree as well as research purpose and the University of Dodoma for providing facilities to carry out this study in its Computational Chemistry Laboratory.

References

[1] G. Pepe, J. M. Cole, P. G. Waddell, and J. R. D. Griffiths, "Molecular engineering of fluorescein dyes as complementary absorbers in dye co-sensitized solar cells," *Molecular Systems Design & Engineering*, vol. 1, no. 4, pp. 402–415, 2016.

[2] W. A. Farooq, A. Fatehmulla, F. Yakuphanoglu et al., "Photovoltaic characteristics of solar cells based on nanostructured titanium dioxide sensitized with fluorescein sodium salt," *Theoretical and Experimental Chemistry*, vol. 50, no. 2, pp. 121–126, 2014.

[3] L. M. Gonçalves, V. de Zea Bermudez, H. A. Ribeiro, and A. M. Mendes, "Dye-sensitized solar cells: a safe bet for the future," *Energy & Environmental Science*, vol. 1, no. 6, p. 655, 2008.

[4] J. Zhang, H. B. Li, S. L. Sun, Y. Geng, Y. Wu, and Z. M. Su, "Density functional theory characterization and design of high-performance diarylamine-fluorene dyes with different π spacers for dye-sensitized solar cells," *Journal of Materials Chemistry*, vol. 22, no. 2, pp. 568–576, 2012.

[5] M. Bourass, A. T. Benjelloun, M. Benzakour et al., "The computational study of the electronic and optoelectronics properties of new materials based on thienopyrazine for application in dye solar cells," *Journal of Materials and Environmental Science*, vol. 7, pp. 700–712, 2016.

[6] S. Mathew, A. Yella, P. Gao et al., "Dye-sensitized solar cells with 13% efficiency achieved through the molecular engineering of porphyrin sensitizers," *Nature Chemistry*, vol. 6, no. 3, pp. 242–247, 2014.

[7] A. Mishra, M. K. R. Fischer, and P. Bäuerle, "Metal-free organic dyes for dye-sensitized solar cells: from structure: property relationships to design rules," *Angewandte Chemie International Edition*, vol. 48, no. 14, pp. 2474–2499, 2009.

[8] B. H. S. T. da Silva, B. A. Bregadiolli, C. F. de Oliveira Graeff, and L. C. da Silva-Filho, "$NbCl_5$-promoted synthesis of fluorescein dye derivatives: spectroscopic and spectrometric characterization and their application in dye-sensitized solar cells," *ChemPlusChem*, vol. 82, no. 2, pp. 261–269, 2017.

[9] C. Lee, W. Yang, and R. G. Parr, "Development of the Colle-Salvetti correlation-energy formula into a functional of the electron density," *Physical Review B*, vol. 37, no. 2, pp. 785–789, 1988.

[10] F. Santoro, A. Lami, R. Improta, J. Bloino, and V. Barone, "Effective method for the computation of optical spectra of large molecules at finite temperature including the Duschinsky and Herzberg–Teller effect: the Q_x band of porphyrin as a case study," *The Journal of Chemical Physics*, vol. 128, no. 22, article 224311, 2008.

[11] A. El Assyry, R. Jdaa, B. Benali, M. Addou, and A. Zarrouk, "Optical and photovoltaic properties of new quinoxalin-2(1H)-one-based D-A organic dyes for efficient dye-sensitized solar cell using DFT," *Journal of Materials and Environmental Science*, vol. 6, no. 9, pp. 2612–2623, 2015.

[12] T. Marinado, K. Nonomura, J. Nissfolk et al., "How the nature of triphenylamine-polyene dyes in dye-sensitized solar cells affects the open-circuit voltage and electron lifetimes," *Langmuir*, vol. 26, no. 4, pp. 2592–2598, 2010.

[13] F. Agda, T. Abram, M. Taleb, L. Bejjit, and M. Bouachrine, "DFT investigations on optoelectronic properties of new low gap compounds based on carbazol and thiophene as solar cells materials," *Journal of Chemistry and Materials Research*, vol. 4, pp. 6–12, 2015.

[14] P. F. Barbara, T. J. Meyer, and M. A. Ratner, "Contemporary issues in electron transfer research," *The Journal of Physical Chemistry*, vol. 100, no. 31, pp. 13148–13168, 1996.

[15] F. De Angelis, S. Fantacci, and A. Selloni, "Alignment of the dye's molecular levels with the TiO_2 band edges in dye-sensitized solar cells: a DFT–TDDFT study," *Nanotechnology*, vol. 19, no. 42, article 424002, 2008.

[16] G. Pourtois, D. Beljonne, J. Cornil, M. A. Ratner, and J. L. Brédas, "Photoinduced electron-transfer processes along molecular wires based on phenylenevinylene oligomers: a quantum-chemical insight," *Journal of the American Chemical Society*, vol. 124, no. 16, pp. 4436–4447, 2002.

[17] C.-P. Hsu, "The electronic couplings in electron transfer and excitation energy transfer," *Accounts of Chemical Research*, vol. 42, no. 4, pp. 509–518, 2009.

[18] R. A. Marcus, "Electron transfer reactions in chemistry. Theory and experiment," *Reviews of Modern Physics*, vol. 65, no. 3, pp. 599–610, 1993.

[19] J. B. Asbury, Y. Q. Wang, E. Hao, H. N. Ghosh, and T. Lian, "Evidences of hot excited state electron injection from sensitizer molecules to TiO_2 nanocrystalline thin films," *Research on Chemical Intermediates*, vol. 27, no. 4-5, pp. 393–406, 2001.

[20] R. Katoh, A. Furube, T. Yoshihara et al., "Efficiencies of electron injection from excited N3 dye into nanocrystalline semiconductor (ZrO_2, TiO_2, ZnO, Nb_2O_5, SnO_2, In_2O_3) films," *The Journal of Physical Chemistry B*, vol. 108, no. 15, pp. 4818–4822, 2004.

[21] N. S. Babu and D. Jayaprakash, "Global and reactivity descriptors studies of cyanuric acid tautomers in different solvents by using of density functional theory (DFT)," *International Journal of Science and Research*, vol. 4, no. 6, pp. 615–620, 2015.